RADIO-FREQUENCY HEATING IN STRAIGHT FIELD LINE MIRROR NEUTRON SOURCE

V. E. Moiseenko[1,2], O. Ågren[1], and K. Noack[1]

[1]*Division of Electricity and Lightning Research, Ångström Laboratory, Uppsala University, Box 534, SE-751 21 Uppsala, Sweden*

[2]*Institute of Plasma Physics, National Science Center "Kharkiv Institute of Physics and Technology", 61108 Kharkiv, Ukraine*

There is a need in a practical scenario for ion heating up to high temperatures in a mirror based neutron source. Such a scenario could be developed with the ion cyclotron heating. Fundamental harmonic ion cyclotron heating of deuterium and second harmonic heating for tritium are studied numerically from the point of view of antenna coupling and heating efficiency. The behavior of the antenna loading resistance and radio-frequency power shine-through the cyclotron zone with the heating frequency, plasma density and temperature and the antenna position is analyzed.

I. INTRODUCTION

In Ref. 1 a scheme is proposed for a sub-critical fast nuclear reactor driven by powerful fusion neutron source based on the straight field line mirror (SFLM[2]). Fusion neutrons are generated in plasma with hot deuterium and tritium ions. There is also a small portion of hydrogen plasma confined between electric potential barriers serving as a stabilizer for the cone instabilities. The high energy of the deuterium and tritium is sustained by radio-frequency (RF) heating.

The scenario chosen for heating of hydrogen isotopes is similar to the scenarios previously developed for the fusion reactor SFLM studies in Refs. 3 and 4. To heat the deuterium ion component, the fundamental harmonic of the ion cyclotron resonance is used. This heating starts first. When deuterium becomes hot it gives some energy to tritium ions via Coulomb collisions. After this, a second harmonic heating of tritium can be started.

The SFLM neutron source has a substantially smaller size than a fusion reactor machine. In this situation the fast magnetosonic wave which is excited by the antenna makes fewer oscillations across the magnetic field. The width of the ion cyclotron zone becomes smaller owing to the sharper gradients of the magnetic field magnitude along magnetic field lines. The last factor is softened by a smaller mirror ratio.

The RF heating in the SFLM neutron source is simulated using the numerical model presented in Ref. 4. The antenna chosen is similar to the one modeled in that paper: a single segmented strap oriented along the plasma boundary perpendicular to the steady magnetic field and minor elliptic axis of the plasma cross-section.

II. NUMERICAL MODEL AND PARAMETERS OF CALCULATIONS

The electromagnetic calculations are performed for a straight field line mirror device, schematically shown in Fig. 1.

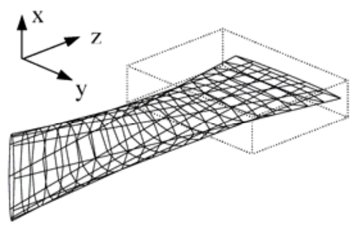

Fig. 1. Sketch of SFLM with calculation domain.

The magnetic field strength of that device is described by the following formula:

$$\mathbf{B}_0 = B_{00}\left[\frac{\mathbf{e}_z}{1-z^2/c^2} - \mathbf{e}_x \frac{x}{c}\frac{1+z/c}{(1-z^2/c^2)^2} + \mathbf{e}_y \frac{y}{c}\frac{1-z/c}{(1-z^2/c^2)^2}\right]$$

where c is the half-distance between the left and right poles of the trap. At the poles at $z=\pm c$, the magnetic field strength goes to infinity. In the numerical model, the plasma diamagnetism is included by adding the finite beta correction to the magnetic field from a prescribed pressure distribution, i.e. $\mathbf{B} = \mathbf{B}_0\sqrt{1-\beta}$. We consider a trap with $c = 12$ m, $a = 40$ cm and $B_0 = 2$ T. Here, a is the plasma radius at the central plane where the magnetic surfaces have a circular cross-section. We choose the ends of the trap at $z = \pm 0.75c$ (where the local mirror ratio is

2.3). The computation domain is $z \in (0.6c, 0.75c)$, i.e. 7.2 m < z < 9 m. As in Refs. 3 and 4 we neglect the B_y component of the steady magnetic field, which only slightly effects the RF heating.

In the model of RF heating of sloshing ions, the above-mentioned segment of the plasma column is surrounded by a rectangular metallic box with one open side at $z = 7.2$ m and with sizes $L_x = 40$ cm, $L_y = 150$ cm and $L_z = 180$ cm.

For calculation of the electromagnetic fields, the zero electron mass approximation is chosen in which the parallel component of the electric field is neglected in Maxwell's operator,

$$\nabla \times \nabla \times \left(\mathbf{E} - \mathbf{e}_\| \mathbf{e}_\| \cdot \mathbf{E}\right) - k_0^2 \hat{\boldsymbol{\varepsilon}} \cdot \mathbf{E} = i\omega\mu_0 \mathbf{j}_{ext} , \tag{1}$$

where $\mathbf{e}_\| = \mathbf{B}/B$ and $\mathbf{j}_{ext}$ is the antenna electric current density. This approximation describes correctly the propagation and absorption of the fast waves and is advantageous for the implementation of the numerical methods. The boundary condition at a metallic surface is

$$\mathbf{E} \times \mathbf{n} = 0 ,$$

where $\mathbf{n}$ is the normal vector of the surface. The boundary condition at the left end of the box at $z = 7.2$ m is chosen as

$$\frac{\partial}{\partial z}(\mathbf{E} \times \mathbf{e}_z) + ik_w(\mathbf{E} \times \mathbf{e}_z) = 0 , \tag{2}$$

where k_w is a constant. This boundary condition is dissipative. It is aimed to model single-path damping of the wave that is launched to the central part of the trap that is located outside the computational region.

The cold plasma dielectric tensor is reasonably accurate to describe the fast wave propagation in fusion plasma far from the cyclotron resonances. Near the fundamental ion cyclotron resonance the thermal corrections caused the particle motions along magnetic field lines become important for the resonant component of the dielectric displacement vector $D_+ = \mathbf{e}_+^* \cdot \mathbf{D}$ (here $\mathbf{e}_+ = (\mathbf{e}_\tau + i\mathbf{e}_y)/\sqrt{2}$ and $\mathbf{e}_\tau = \mathbf{e}_y \times \mathbf{e}_\|$). Its dependence on the electric field is non-local[5]

$$D_+ = \varepsilon_0 \int_{-L_L}^{L_R} \tilde{\varepsilon}_{++}(l, l') E_+(l') dl' , \tag{3}$$

where l is the coordinate along magnetic field line, L_L and L_R correspond to its left and right ends. In the WKB limit the following expression could be used for the kernel of the integral in (3) (see Ref. 5):

$$\tilde{\varepsilon}_{++} = \varepsilon_{++}\delta(l - l') + 2\,\mathrm{Im}\,\varepsilon_{++}\,\delta(l + l' - l_{res})\,\eta(\mathbf{k} \cdot \mathbf{e}_\| \nabla B \cdot \mathbf{e}_\|) , \tag{4}$$

where $\varepsilon_{++} = 1 - \sum_\alpha \frac{\omega_{p\alpha}^2}{\omega |k_\| v_{T\|\alpha}|} \left[F(\beta_\alpha) - \frac{i\sqrt{\pi}}{2} \exp(-\beta_\alpha^2) \right]$, η is the Heaviside function, F is the Dawson integral, $\beta_\alpha = (\omega - \omega_{c\alpha}) / |k_\| v_{T\|\alpha}|$ and l_{res} is the cyclotron resonance point. The second term in formula (4) is non-zero only for the wave traveling to higher magnetic field. Since in our heating scenario the fast wave is launched in the opposite direction, we drop this term.

The second harmonic ion cyclotron resonance reveals up if the electromagnetic field is non-uniform across the magnetic field lines. In the WKB limit the corresponding contribution to the resonant component of the displacement vector can be calculated by the finite Larmor radius expansion

$$\delta\mathbf{D}/\varepsilon_0 = -\frac{1}{8}\mathbf{e}_\| \times \mathbf{e}_\| \times \left[\nabla_\perp \cdot \left(\tilde{\varepsilon}_{+2}\nabla_\perp\right)\right]\mathbf{E}_+$$

$$-\frac{1}{8} i\mathbf{e}_\| \times \left[\nabla_\perp \cdot \left(\tilde{\varepsilon}_{+2}\nabla_\perp\right)\right]\mathbf{E}_+ - \frac{1}{4}\nabla\tilde{\varepsilon}_{+2} \cdot \left(\mathbf{e}_\| \times \nabla\right)\mathbf{E}_+$$

where $\nabla_\perp = \nabla - \mathbf{e}_\| \mathbf{e}_\| \cdot \nabla$,

$$\mathbf{E}_+ = -\frac{1}{2}\mathbf{e}_\| \times \mathbf{e}_\| \times \mathbf{E} - \frac{i}{2}\mathbf{e}_\| \times \mathbf{E} ,$$

$$\tilde{\varepsilon}_{+2} = \sum_\alpha \frac{4\omega_{p\alpha}^2 v_{T\perp\alpha}^2}{\omega |k_\| v_{T\|\alpha}| \omega_{c\alpha}^2} \left[F(\beta_{2\alpha}) - \frac{i\sqrt{\pi}}{2}\exp(-\beta_{2\alpha}^2) \right] \times$$

$$\left[1 + (1 - 2\omega_{c\alpha}/\omega)(v_{T\perp\alpha}^2 / v_{T\|\alpha}^2 - 1)\right]$$

and $\beta_{2\alpha} = (\omega - 2\omega_{c\alpha}) / |k_\| v_{T\|\alpha}|$.

For the fundamental cyclotron harmonic heating of deuterium and for the second harmonic heating of tritium we consider the same antennas similar as in Refs. 3 and 4. They are aimed to excite waves with small k_y . We choose the antenna height as $l_x = 9$ cm, the antenna width as $l_z = 10$ cm and the antenna length as $l_y = 130$ cm. The regular position of the antenna with respect to the center of the trap is $z_a = 845$ cm.

In the numerical calculations, the following regular set of parameters is chosen: Plasma density (in its maximum) is $n_{e0} = 10^{14}$ cm^{-3}, heating frequency is $\omega = 1.1 - 2.1 \cdot 10^8$ s^{-1}, deuterium and tritium parallel and perpendicular thermal velocities at the z -axis are $v_{T\|D} = v_{T\|T} = 5 \cdot 10^5$ m/s and $v_{T\perp D} = v_{T\perp T} = 1.35 \cdot 10^6$ m/s, the deuterium concentration is $C_D = 0.4$, $k_\| = 0.2$ cm^{-1} and $k_w = 0.15$ cm^{-1}.

III. FUNDAMENTAL HARMONIC DEUTERIUM HEATING

The frequency scan for fundamental harmonic heating is presented in Fig. 2. There the antenna loading (absorption) resistance $r_{pl} = 2P_{dis}/I^2$, a characteristic of the antenna heating efficiency, is plotted. Here

$$P_{tot} = P_{dis} + P_{fl} , \tag{5}$$

and $P_{dis} = \int \left(p_{+2} + \frac{\omega \varepsilon_0}{2} |E_+|^2 \operatorname{Im} \varepsilon_{++} \right) dV$ is the power dissipated in the plasma, $P_{fl} = \int (\mathbf{\Pi} + \mathbf{\Pi}_{+2}) \cdot d\mathbf{s}$ is the power leakage owing to the dissipative boundary condition (2), $\mathbf{\Pi}$ is the Poynting vector, $\mathbf{\Pi}_{+2}$ is the kinetic energy flux and I is the current in the antenna. According to the formula (5) we split the antenna loading resistance into the parts $r_{tot} = r_{pl} + r_{fl}$. r_{fl} is shown in the figure by a dashed curve.

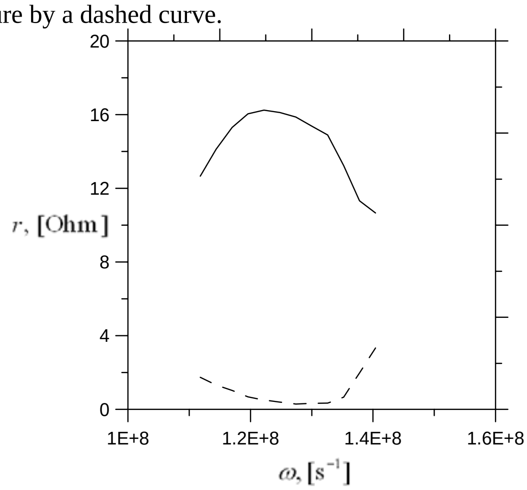

Fig. 2. Dependence of the absorption (solid line) and shine-through (dashed line) resistances on RF heating frequency.

In the range of frequencies $\omega = 1.15 - 1.35 \cdot 10^8 \mathrm{s}^{-1}$ the deuterium minority heating is efficient: $r_{pl} >> r_{fl}$ and r_{pl} has a wide maximum. For further calculations, the regular frequency is chosen as $\omega = 1.3 \cdot 10^8 \mathrm{s}^{-1}$.

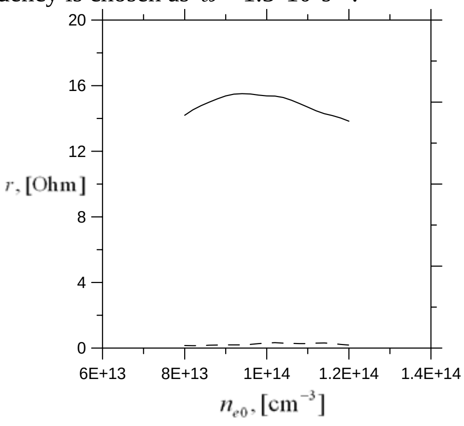

Fig. 3. Dependence of the absorption and shine-through resistances on plasma density.

Fig. 3 shows the dependence of the above mentioned resistances of plasma density. In this plot, there is a broad maximum of r_{pl} again and r_{fl} is kept small. The dependence of r_{pl} on k_w, the free parameter of the model, is expectably small because almost all RF power is absorbed by plasma before it reaches the left boundary.

The dependence on the antenna position along the magnetic trap is also not sensitive (see Fig.4). The drop of r_{pl} at long distances is associated with decrease of antenna-plasma coupling. The dependence on the perpendicular ion temperature is also calculated. It is weak in the temperature range 40-80 keV.

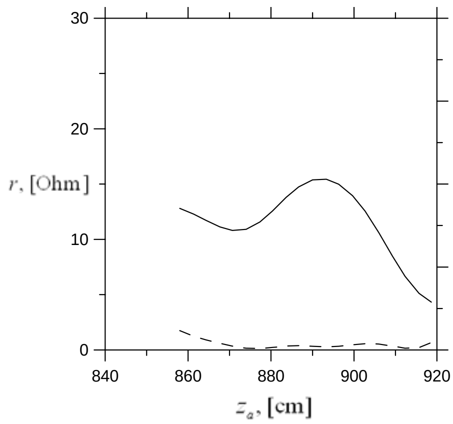

Fig. 4. Dependence of the absorption and shine-through resistances on antenna location.

IV. SECOND HARMONIC TRITIUM HEATING

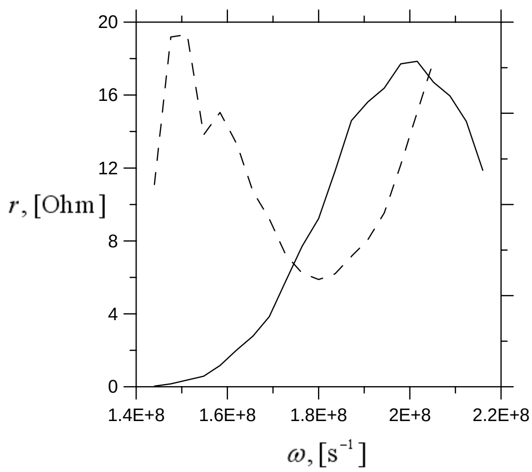

Fig. 5. Dependence of the second harmonic absorption and shine-through resistances on RF heating frequency.

For the second harmonic tritium heating the wave damping is not strong and the shine-trough of the RF power to the middle part of the device is noticeable. The best ratio of the absorption resistance r_{pl} to the shine-through resistance r_{fl} is for the frequency $\omega = 1.9 \cdot 10^8 \mathrm{s}^{-1}$. The RF power penetrated to the central part of the trap would be damped there at the deuterium second harmonic resonance and in this sense is not wasted. The plasma density dependence (see Fig. 6) is much more sensitive than in fundamental harmonic case. This is because of the wave damping increases both with $k_{\parallel}$ and $k_{\perp}$.

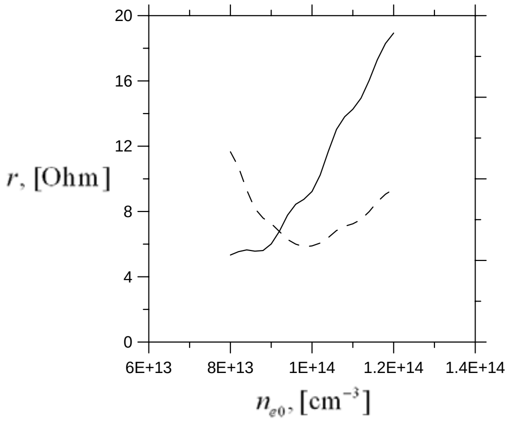

Fig. 6. Dependence of the second harmonic absorption and shine-through resistances on plasma density.

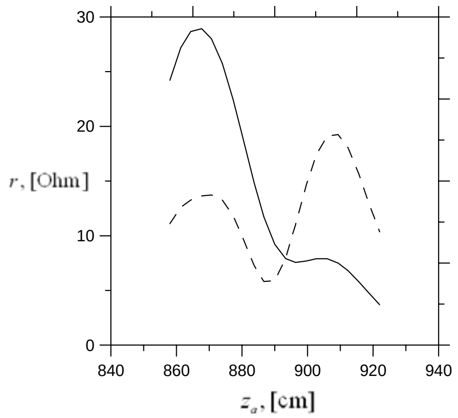

Fig. 7. Dependence of the second harmonic absorption and shine-through resistances on antenna location.

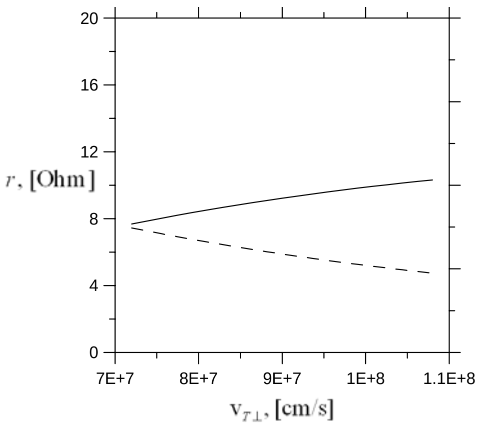

Fig. 8. Dependence of the second harmonic absorption and shine-through resistances on tritium thermal velocity.

The variation of antenna location (see Fig. 7) prompts that the antenna should be placed closer to the midplane. However, this is not desirable because of the high neutron flux. If antenna is placed at the distance $z_a = 900 - 910$ cm from the midplane it couples to the first radial mode of the fast magnetosonic wave. Because of low $k_{\perp}$, this mode is damped more weakly and has a tendency to shine-through. At bigger distance, antenna-plasma coupling decreases.

Fig.8 indicates that the wave damping increases with the perpendicular thermal ion velocity in the case of second harmonic heating. As well as in the case of fundamental harmonic, the dependence of r_{pl} on k_w, is small.

V. SUMMARY

The calculations show good performance of deuterium minority heating at fundamental ion cyclotron frequency. The heating is weakly sensitive to the ion temperature and, therefore, has no start-up problem. The sensitivity to other factors, e.g. plasma density, antenna location etc., is not critical. The second harmonic heating of tritium is more delicate. It is every time accompanied by a noticeable shine-through of the wave energy to the middle part of the trap where the wave would be absorbed by the deuterium at the second harmonic ion cyclotron zone. Most of the remaining wave energy may also be absorbed at the second harmonic tritium resonance zone near the opposite mirror. The calculations predict relatively sensitive dependence on plasma density, antenna location and tritium temperature. However, if the necessary conditions are provided this heating is satisfactorily efficient.

ACKNOWLEDGMENTS

The Swedish Institute support is acknowledged.

REFERENCES

1. O. ÅGREN, V.E. MOISEENKO, K. NOACK, A. HAGNESTÅL, *Fusion Science and Technology*. **55**, no. 2T, 46 (2009).
2. O. ÅGREN AND N. SAVENKO, *Phys. Plasmas* **12**, ID 022506 (2005).
3. V.E. MOISEENKO, O. ÅGREN, *Phys. Plasmas* **12**, ID 102504 (2005).
4. V.E. MOISEENKO, O. ÅGREN, *Phys. Plasmas* **14**, ID 022503 (2007).
5. S.V. KASILOV, A.I. PYATAK, K.N. STEPANOV, “Nonlocal theory of cyclotron and Cerenkov absorption in nonuniformly magnetized plasma”, In: *Reviews of Plasma Physics* Vol. 20, p. 61, Consultants Bureau, New York-London (1997).